

# Imaging Atrial Septal Defects by Real-Time 3D Transesophageal Echocardiography: Step-by-Step Approach

Muhammed Saric, MD, PhD, FASE, Gila Perk, MD, FASE, Jan R. Purgess, MD,  
and Itzhak Kronzon, MD, FASE, *New York, New York*

**Background:** There are currently no standardized three-dimensional (3D) transesophageal echocardiographic (TEE) views of the interatrial septum and atrial septal defects (ASDs). Without a standardized approach, it is difficult to ascertain the important anatomic relationships (such as the location of the aortic rim of an ASD), to perform relevant measurements (such as the size of an ASD or the size of its rims), or to guide the deployment of catheters and devices during atrial septal closure.

**Methods:** Using a 3D TEE matrix-array transducer, 706 TEE studies were performed over a 14-month period. The purpose of the study was to develop a standardized protocol for anatomically correct orientation of 3D TEE images of the interatrial septum and ASDs.

**Results:** Among 706 TEE studies, there were 23 patients with ASDs, representing 3.3% of the study population. Eighteen patients had secundum ASDs, two had primum ASDs, and three had sinus venosus ASDs of the superior vena cava. A protocol for properly orienting 3D TEE images of the interatrial septum and ASDs was developed. When the images are acquired at an angle of 0°, the septum is properly oriented by the tilt-up-then-left maneuver. The initial 3D TEE image is first tilted up to reveal the right atrial side of the septum. Then the image is tilted 180° around its vertical axis to reveal the left atrial side of the septum; the aortic rim is on the left, the superior vena cava on the top, and the right-sided pulmonary vein ostia on the right side of the screen. For acquisitions at a higher angle, the rotate-left-in-z-axis maneuver is used. The image is first tilted up to reveal the right atrial side of the septum, as in the tilt-up-then-left maneuver. The image is then rotated counterclockwise in the z axis until the superior vena cava is at 12 o'clock. Finally, the image is tilted 180° around its vertical axis to reveal the left atrial side of the septum.

**Conclusions:** The use of standardized tilt-up-then-left and rotate-left-in-z-axis maneuvers enhances the diagnosis of ASDs, ascertains the important anatomic relationships of ASDs to surrounding structures, and facilitates communication between echocardiographers obtaining 3D TEE images and interventional cardiologists or cardiac surgeons performing ASD closures. (*J Am Soc Echocardiogr* 2010; ■:■-■.)

**Keywords:** Real-time three-dimensional echocardiography, Transesophageal, Atrial septal defect, Interatrial septum, Device closure

Three-dimensional (3D) transesophageal echocardiographic (TEE) imaging has been revolutionized by the introduction of a 3D-TEE probe with a matrix-array transducer with 3,000 elements. This is approximately a 50-fold increase in the number of imaging elements compared with a standard two-dimensional transesophageal echocar-

From the Division of Cardiology, New York University Langone Medical Center, New York, New York (M.S., G.P., I.K.); and the Department of Anesthesiology, New York University School of Medicine and New York Veterans Affairs Hospital, New York, New York (J.R.P.).

Dr. Kronzon receives speakers' bureau honoraria from Philips Medical Systems (Andover, MA).

Reprint requests: Muhammed Saric, MD, PhD, FASE, New York University Medical Center, Noninvasive Cardiology Laboratory, 560 First Avenue, New York, NY 10016 (E-mail: [muhammed.saric@nyumc.org](mailto:muhammed.saric@nyumc.org)).

0894-7317/\$36.00

Copyright 2010 by the American Society of Echocardiography.

doi:10.1016/j.echo.2010.08.008

diographic probe, which typically has 64 elements. The basic principles and history of 3D echocardiography have been presented in detail elsewhere.<sup>1-3</sup>

What is the major difference between 2D and 3D TEE image acquisition? Briefly, a 2D TEE probe acquires a sector image whose dimensions are as follows: width of up to 90° in the lateral (azimuth) direction, depth of up to approximately 16 cm in the axial direction, and thickness (elevation) that is negligible. The 3D TEE matrix-array probe expands this concept by acquiring not just one but a series of 2D sector images along the elevation axis to create a 3D pyramidal data set referred to as a frustum. By convention, the lateral (azimuth) direction is encoded in red, the elevation direction in green, and the depth direction in blue.

Aside from the three axes of the pyramidal data set itself, there are also three axes of the 2D image used to display the pyramidal set on the screen. The horizontal axis runs from the left to the right edge of the screen. The vertical axis runs from the top to the bottom of the screen. Additionally, the axis that is perpendicular to the computer

62  
63  
64  
65  
66  
67  
68  
69  
70  
71  
72  
73  
74  
75  
76  
77  
78  
79  
80  
81  
82  
83  
84  
85  
86  
87  
88  
89  
90  
91  
92  
93  
94  
95  
96  
97  
98  
99  
100  
101  
102  
103  
104  
105  
106  
107  
108  
109  
110  
111  
112  
113  
114  
115  
116  
117  
118  
119  
120  
121  
122

## Abbreviations

ASD = Atrial septal defect

IVC = Inferior vena cava

ROLZ = Rotate-left-in-z-axis

SVC = Superior vena cava

TEE = Transesophageal  
echocardiographic

3D = Three-dimensional

TUPLE = Tilt-up-then-left

2D = Two-dimensional

monitor on the ultrasound system and comes out of the screen toward the user at the time of image review is referred to as the z axis. Rotations along the z axis move in clockwise or counterclockwise direction and allow for placing 3D images into conventional views (such as the surgical view of the mitral valve or the anatomic orientation of the interatrial septum).

There are currently no standardized 3D TEE views of the interatrial septum and atrial septal

defects (ASDs). Without a standardized approach, it is difficult to ascertain the important anatomic relationships (such as the location of the aortic rim of an ASD), to perform relevant measurements (such as the size of the ASD or the size of its rims), or to guide the deployment of catheters and devices during atrial septal closure.

The purpose of this study was to develop a standardized protocol for the placement of 3D TEE images in anatomically correct orientation.

## METHODS

Three-dimensional TEE studies were recorded with a commercially available ultrasound system (Philips iE33; Philips Medical Systems, Andover, MA) using a matrix-array 3D TEE probe (X7-2 t; Philips Medical Systems). Over a 14-month period, 3D TEE studies were performed in 706 individuals.

Three-dimensional TEE images were obtained in the following four modalities: (1) biplane imaging (a side-by-side display of a pair of 2D TEE images that are 90° apart), (2) full-volume imaging (the frustum is automatically subdivided by the ultrasound system in several slices; each slice is acquired over one cardiac cycle; individual slices are stitched together and displayed in a delayed nonlive fashion), (3) narrow-angle live 3D imaging (live imaging of a system-selected frustum segment measuring approximately 60° × 30° in lateral x elevation axes and having a full depth in the depth axis), and (4) wide-angle 3D zoom imaging (live imaging of a user-selected frustum segment measuring up to 85° × 85° in lateral x elevation axes but with a system-limited slice thickness in the depth axis).

Wide-angle 3D zoom appears to be the most useful 3D modality for visualizing the anatomy of the interatrial septum because it provides instantaneous (live) images of almost the entire interatrial septum. Although full-volume 3D imaging provides a wider view of the interatrial septum than the 3D zoom, it is not instantaneous and often suffers from stitching artifacts (misalignment of image slices obtained in separate cardiac cycles). Narrow-angle live 3D imaging is used extensively during percutaneous atrial septal closure procedures to visualize the tips and trajectories of various catheters and devices used in closing defects.<sup>4</sup>

With reference to the manipulation of the 3D image on the ultrasound system, the word "tilt" is used in this report to refer to image movements around either the horizontal or the vertical axis of the image and the word "rotation" to refer to image movements in the z axis.

Because the raw 3D TEE images are often nonintuitive, a standardized approach for image acquisition and display of the interatrial septum and ASDs is needed. In this article, we propose two simple

maneuvers for rapid orientation of 3D TEE images of the interatrial septum in proper anatomic orientations.

## RESULTS

Among 706 3D TEE studies performed, we identified 23 patients with ASDs (3.3% of the study population). There were 18 patients with secundum ASDs, two with primum ASDs, and three with sinus venosus ASDs of the superior vena cava (SVC). After a trial-and-error optimization, we developed a simple protocol for the placement of 3D TEE images of the interatrial septum in anatomically correct orientation. We then used this protocol for imaging a variety of ASDs.

## Protocol Development

Preparations for 3D TEE imaging start with the acquisition of good 2D TEE images of the interatrial septum. In principle, the interatrial septum can be imaged at any 2D angle. Image acquisition at 0° and 90° is described first. Then the impact of image acquisition at intermediate 2D angles on the subsequent 3D TEE images is discussed. All image acquisition described in this article were performed on 3D TEE systems from Philips Medical Systems. However, the general principles should apply to 3D TEE systems that are being developed by other manufacturers.

**Image Acquisition at 0° (Tilt-Up-Then-Left [TUPLE] Maneuver).**

After obtaining a good midesophageal view of the interatrial septum at 0° in 2D mode, the 3D zoom mode is selected. Initially, a pair of biplane images appears on the screen. The left image represents the lateral (azimuth or red) plane, while the right image represents the elevation (green) plane. In each image, there is a region-of-interest selection box; the user can select the sector width in azimuth or elevation planes by changing the left and right borders of the box using the track ball. Additionally, by moving the selection box up and down the screen, the user determines which portion of the depth (blue) plane will be displayed in the subsequent 3D view.

After the region of interest is selected, the 3D zoom view is obtained. The image of the interatrial septum appears in the same orientation as the 2D image at 0° (Figure 1A); that is, the interatrial septum is seen in its long axis rather than en face. We refer to this initial image as the "opening scene."

In the next step, the image is manipulated using to obtain the en face view of the interatrial septum from either the left or the right atrial perspective. This view, which is unobtainable in real time by any imaging technique other than 3D echocardiography, demonstrates the interatrial septum the way an anatomist or a surgeon would view it.<sup>5</sup>

One way to obtain the en face view of the interatrial septum from the opening scene 3D zoom image is to tilt the image down around its horizontal axis. Although this maneuver indeed provides an en face view of the interatrial septum from the left atrial perspective, it places the superior rim of the interatrial septum at the bottom of the screen. In essence, it creates an upside-down image of the interatrial septum (Figure 1B).

Instead, we propose the TUPLE maneuver to provide more intuitive en face images of the interatrial septum. In this maneuver, the initial 3D image of the interatrial septum seen in Figure 1A is first tilted up along its horizontal axis to reveal an en face view of the interatrial septum from the right atrial perspective. The superior portion of the interatrial septum is now on the top of the screen and the anterior portion on the right side of the screen (Figure 1C).

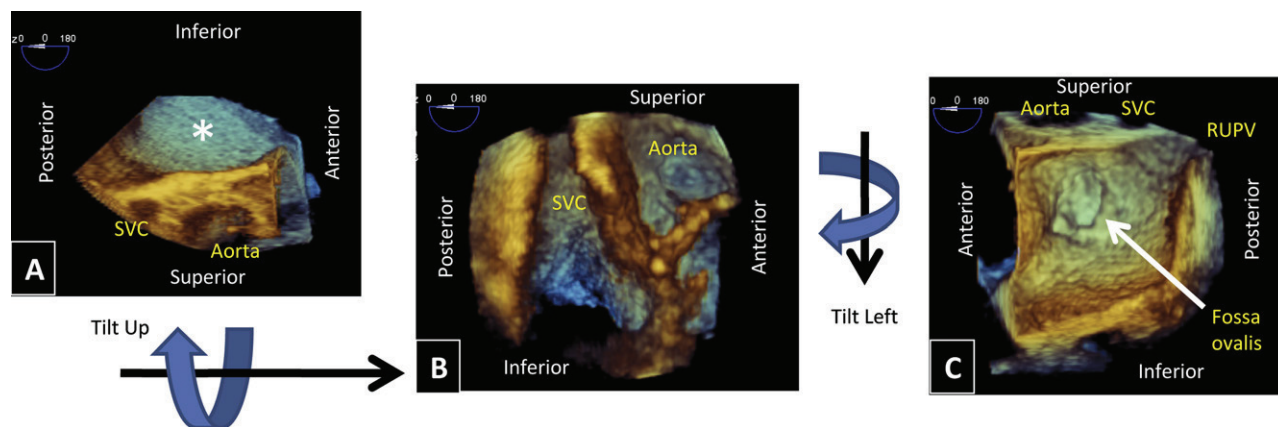


**Figure 1** Imaging of a normal interatrial septum at 0°. **(A)** The initial image (opening scene) of the interatrial septum acquired at 0°. The asterisk denotes the left atrial aspect of the interatrial septum. **(B)** The result of tilting the initial image down to fully reveal the left atrial aspect of the interatrial septum. Such a maneuver places the cranial portion of the interatrial septum counterintuitively to the bottom of the screen. **(C)** The first step of the TUPLE maneuver, namely, tilting up of the image to reveal the right atrial aspect of the interatrial septum. **(D)** The second step of the TUPLE maneuver, namely, tilting of the image along its vertical axis to reveal the left atrial aspect of the interatrial septum in proper anatomic orientation. RUPV, Right upper pulmonary vein.

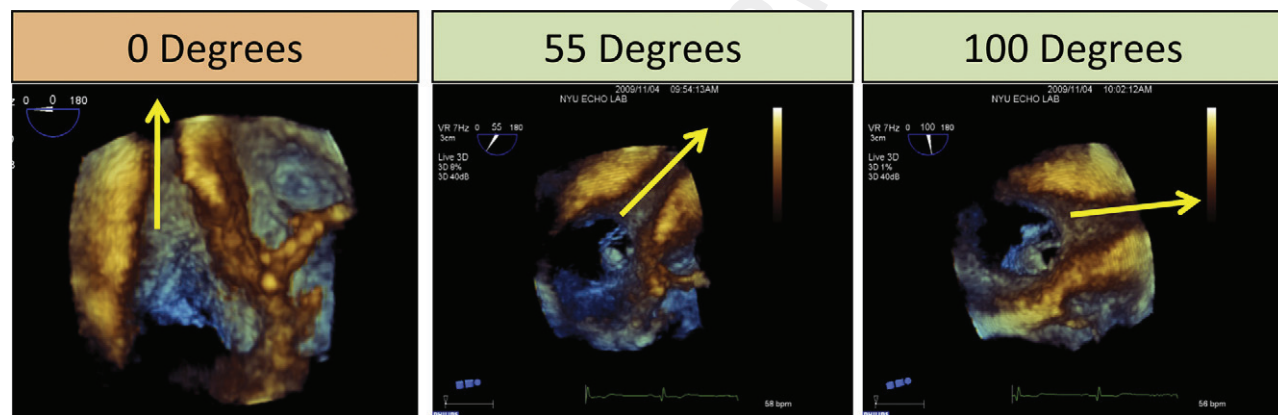


**Figure 2** Imaging at intermediate angles. The impact of various acquisition angles on the 3D images of the interatrial septum is demonstrated. Each image demonstrates the right atrial aspect of the interatrial septum. Note that as the angle of image acquisition increases, the position of the SVC rotates progressively in the clockwise rotation.

The SVC and the ascending aorta are the most important landmark in this view; by identifying and properly orienting these two vessels, one ensures proper orientation of the interatrial septum. The SVC is at the top of the screen, and the aortic valve and the ascending aorta are on the right side of the screen. The fossa ovalis, located in the middle of the image, is another important landmark, because its visualization is essential for guiding transseptal puncture during various percutaneous cardiac interventions.

In the next step, the image of the interatrial septum is tilted to the left around the vertical axis by approximately 180° until the en face view of the interatrial septum from the left atrial perspective is obtained. In this view, the superior rim of the interatrial septum remains at the top of the screen; the anterior (aortic) rim is now on the left side and the ostia of the right-sided pulmonary veins on the right side of the monitor (Figure 1D). The imaging of a normal interatrial septum using the TUPLE maneuver is illustrated in Video 1.

**Image Acquisition at 90° (TUPLE Plus Rotate-Left-in-z-Axis [ROLZ] Maneuver).** Using the same principle of initial imaging (selection of region of interest in the biplane midesophageal view), the opening scene 3D zoom image is obtained. Again, this initial 3D im-

age has the same orientation as the equivalent 2D image, which represents the bicaval view.

In the first step, the image is tilted up to reveal the right atrial side of the interatrial septum. In comparison with the image obtained at 0°, the SVC now appears on the right side of the screen. In effect, changing the 2D angle at time of image acquisition leads to 3D zoom image rotation in the z axis. Therefore, to orient this 3D image to the proper anatomic position, one must rotate the image to the left (counterclockwise) by 90° in the z axis.

Once the image of interatrial septum from the right atrial perspective properly oriented, it is tilted to the left around its vertical axis to obtain the view of the interatrial septum from the left atrial perspective. We refer to this manipulation of the image as the TUPLE-plus-ROLZ maneuver. It is illustrated in Video 2.

**Imaging at Intermediate Angles.** As a general rule, the larger the 2D angle used at the time of image acquisition, the more rotation of the 3D image in the counterclockwise direction in the z axis will be needed. Images that were acquired at 0° in two dimensions will require no rotation in the z axis of the 3D images, images acquired at 75° will require a 75° counterclockwise rotation in the z axis, images

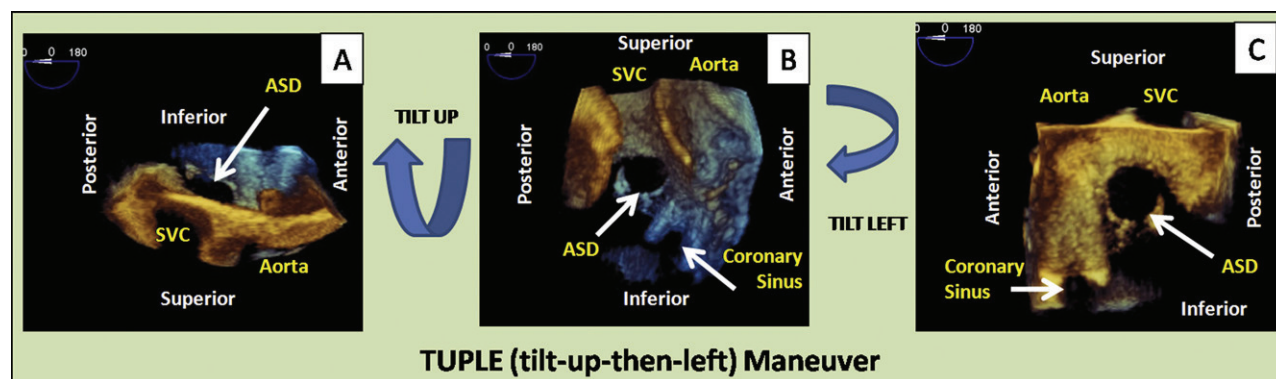


**Figure 3** Imaging of a secundum ASD at 0°. The TUPLE maneuver, described in Figure 2, is here applied to the imaging of a secundum ASD. (A) The initial 3D TEE image (opening scene). (B) The right atrial aspect of the ASD. (C) The left atrial aspect of the ASD.

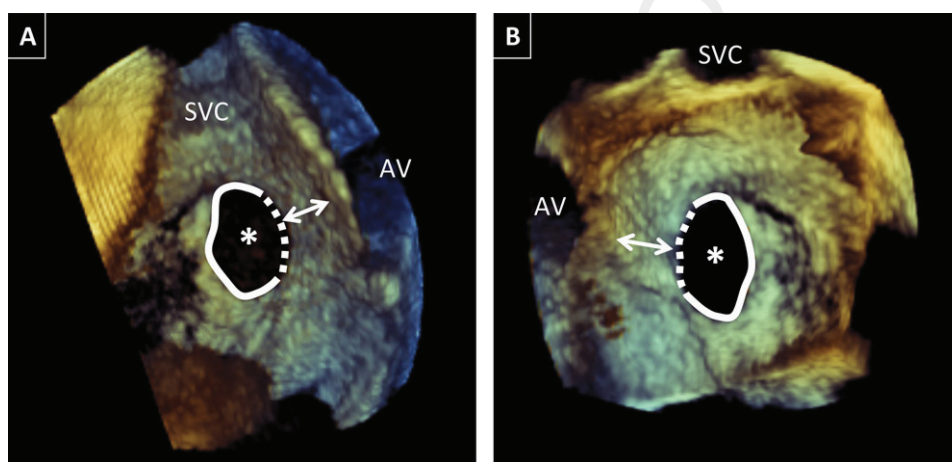


**Figure 4** Rims of a secundum ASD. (A) The right atrial aspect and (B) the left atrial aspect of a secundum ASD (asterisk). The dotted line follows the aortic rim and the solid line follows other rims of the secundum ASD. The size of the aortic rim (arrow) is of utmost importance in percutaneous ASD closure. AV, Aortic valve.

acquired at 100° will require a 100° counterclockwise rotation in the z axis, and so forth. The impact of image acquisition at various 2D angles is shown in Figure 2.

The TUPLE and ROLZ maneuvers were successful in obtaining diagnostic images in all 23 patients with ASDs. On average, the TUPLE maneuver with or without the ROLZ maneuver takes 1 to 2 minutes to perform.

### 3D TEE Imaging of Secundum ASDs

In our series, there were 18 patients with secundum ASDs, 14 of whom were women (72%; all secundum ASDs). Using the TUPLE and ROLZ maneuvers, one places a secundum ASD in the proper anatomic orientation. Figure 3 and Video 3 demonstrate imaging of a secundum ASD using the TUPLE maneuver and a 0° acquisition angle.

Complete resorption of the septum primum over the fossa ovalis leads to the classic appearance of the secundum ASD (Video 4). Three-dimensional TEE imaging clearly demonstrates that these ASDs are frequently not perfectly circular, as has been commonly assumed in 2D echocardiography, but often oval or irregular in shape. In addition, what is assumed to be an ASD's diameter on 2D TEE imaging is often a geometric chord rather than the true ASD diameter. (A geometric chord is a line that connects two points of a circle but does not pass the circle's center, as its diameter does.)

With 3D TEE imaging, one can also appreciate that the size of an ASD varies throughout the cardiac cycle, being maximal during ventricular systole and minimal during atrial systole.<sup>6</sup> In our laboratory, we report the size of the ASD at the time of its maximal diameters. The precise measurement of ASD size helps avoid inappropriate patient selection for percutaneous ASD closure.

A properly oriented 3D TEE image of a secundum ASD allows for evaluation of the size of the ASD tissue rims and their relationship to the aortic valve and the ascending aorta (Figure 4). Knowledge of the defect size and the size of tissue rims is of utmost importance for percutaneous device closure of secundum ASDs. Percutaneous closure of a secundum ASD is usually considered feasible if the largest ASD diameter is <38 mm, its aortic rim is >3 mm, and other rims are >7 mm.<sup>7</sup> Using the TUPLE and ROLZ maneuvers, the location and the size of the each rim in general and the aortic rim in particular can usually be determined.

At present, no measurements of ASD size can be obtained directly from 3D TEE images. Instead, the size of an ASD can be determined (1) semiquantitatively by superimposing a rectangular grid of known dimensions over the 3D TEE ASD image (Figure 5A) and (2) quantitatively by tracing the outlines and diameters of the ASD using offline software for multiplanar reconstruction.

When there is only partial resorption of the septum primum over the fossa ovalis, secundum ASDs appear fenestrated. In such ASDs,

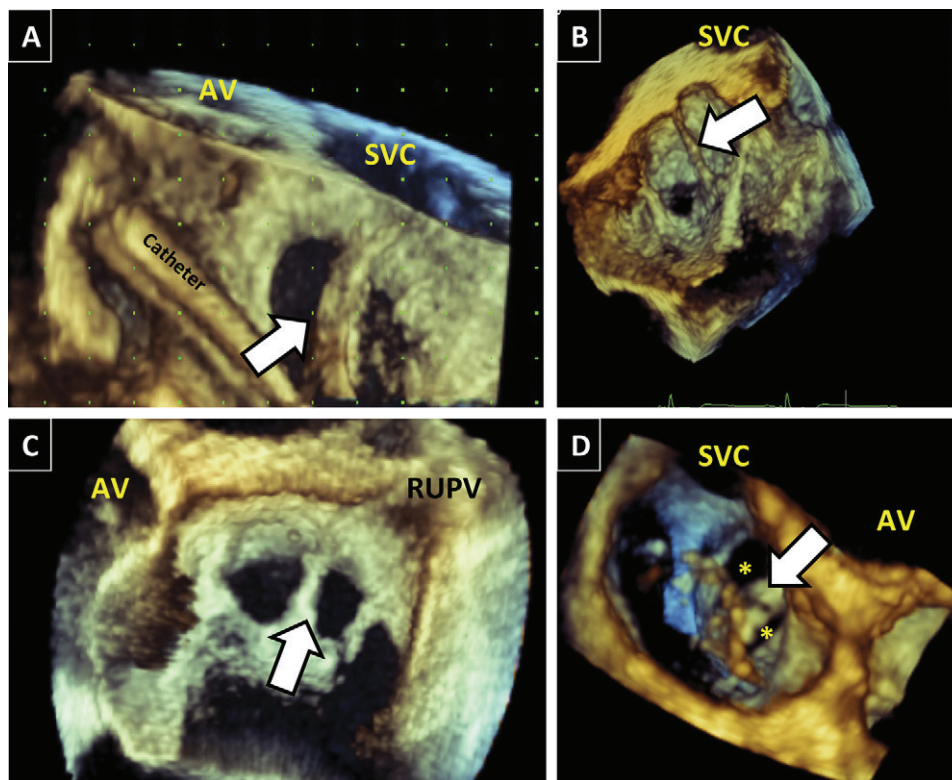


**Figure 5** Fenestrated secundum ASDs. Three-dimensional TEE images of tissue bands (*arrow*) stretched across secundum ASDs (fenestrated ASDs) from four different patients. **(A–C)** Three-dimensional TEE images of ASDs from the left atrial perspective. **(D)** Two ASDs (*asterisks*) separated by a band of tissues as viewed from the right atrial perspective.

there are bands of tissue (remnants of the septum primum) traversing the fossa ovalis.<sup>5</sup> Although the anatomy of such bands is difficult to conceptualize on 2D echocardiography, their appearance is readily ascertained by 3D TEE imaging (Figure 5).

Proper orientation of the 3D TEE images of an ASD, such as through the TUPLE and ROLZ maneuvers, is also essential for guiding the percutaneous device closure of an ASD (Figure 6).

After the septal defect is sized and deemed amenable to percutaneous repair, a collapsed closure device is deployed via the guiding catheter. Three-dimensional TEE imaging allows for continuous visualization of the intracardiac portions of the guiding catheters, balloons, and closure devices.<sup>8</sup>

Once the closure device has been expanded and deployed, 3D TEE imaging is used to ascertain its proper positioning. Both the left atrial and the right atrial plate of the device are easily visualized. In addition, 3D TEE imaging helps determine if sufficient tissue rim is caught between the two plates of the device. In case of device malpositioning, 3D TEE imaging can be used to guide repositioning of the device (Figures 6C and 6D). After the device is fully deployed, 3D TEE color Doppler imaging is used to verify that no significant residual blood flow around the device is present.

### 3D TEE Imaging of Primum ASDs

In general, some 15% of all ASDs are in the region of the ostium primum, located adjacent to the interventricular septum. They are termed primum defects and account for about 15% of all ASDs. Primum ASDs are usually part of the endocardial cushion defect spectrum, ranging from isolated primum ASDs to complete atrioventricu-

lar canal defects. In our series, two patients had primum ASD (1 man, 1 woman).

Using the TUPLE and ROLZ maneuvers, a primum ASD is visualized as an often ovoid communication between the two atria adjacent to the atrioventricular valves. The relationship between a primum ASD and the surrounding structures, such as the mitral and tricuspid valves, is easily discernible from 3D TEE images (Figure 7, Video 5).

Frequently, primum ASDs are associated with a cleft anterior mitral leaflet and the attendant eccentric mitral regurgitation. The anatomy of a cleft leaflet can easily be visualized by 3D TEE imaging from both the atrial and ventricular perspectives (Figures 7C and 7D, Video 6).

### 3D TEE Imaging of Sinus Venosus ASDs

When there is a communication between the sinus venosus portion of the right atrium (which is adjacent to the venae cavae) and the left atrium, the defect is called a sinus venosus ASD. It is more common to observe such a defect adjacent to the ostium of the SVC than the inferior vena cava (IVC). Both sinus venosus ASD types are usually associated with partial anomalous pulmonary venous return.

In an SVC-type sinus venosus ASD, the right upper and the right middle pulmonary vein commonly drain into the SVC instead of the left atrium. In an IVC-type sinus venosus ASD, commonly the lower right pulmonary vein drains into the IVC. Because of the characteristic appearance of the course of this anomalous pulmonary vein on chest x-rays, the condition is referred to as the scimitar syndrome. In general, sinus venosus ASDs account for 5% to 10% of all ASDs. In our series, three patients had primum ASDs (all men).

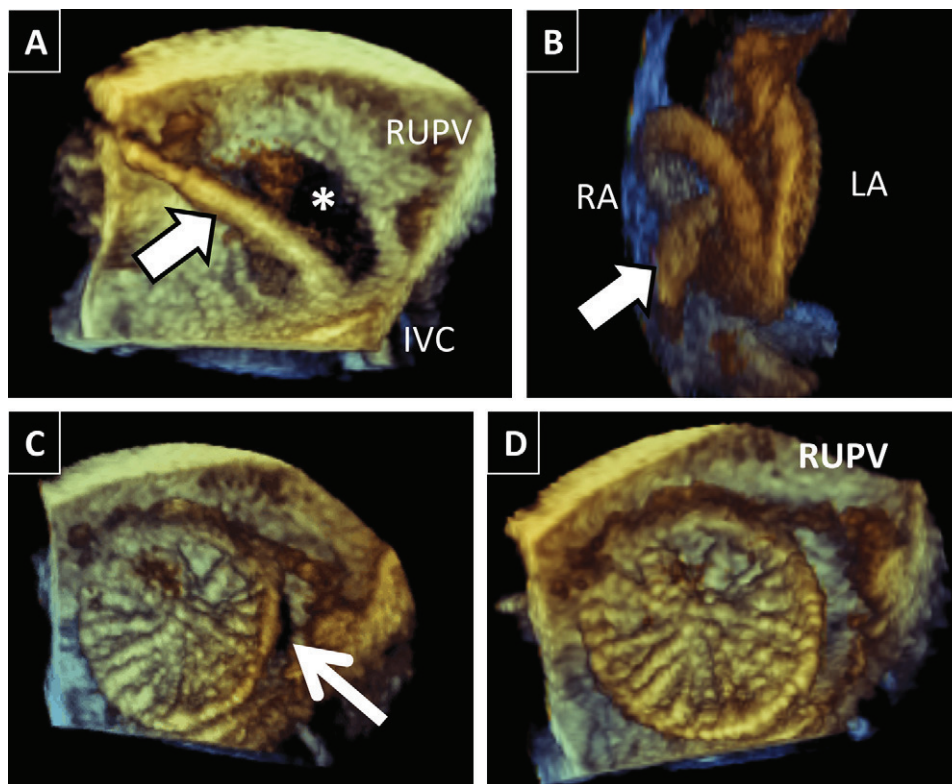


**Figure 6** Percutaneous closure of a secundum ASD. **(A)** The left atrial aspect of the interatrial septum after the TUPLE maneuver. A catheter is being delivered from the IVC through the secundum ASD (asterisk) into the left atrium. **(B)** Cross-section of the interatrial septum. An Amplatzer ASD occluder (AGA Medical, Plymouth, MN) is being delivered to close the secundum ASD; the device is still attached to the delivery catheter (arrow). **(C)** The left atrial disk (LA) of an Amplatzer ASD occluder. Insufficient capture of the posterior ASD rim is noted (arrow). **(D)** The left atrial disk after repositioning; now all the ASD rims are fully captured. RA, Right atrial disk of the ASD occluder; RUPV, right upper pulmonary vein.

Using the TUPLE and ROLZ maneuvers, a sinus venosus ASD is first placed in the correct anatomic orientation and visualized both from the right and left atrial perspectives (Figures 8A and 8B). Video 7 demonstrate an SVC-type sinus venosus ASD with an irregularly shaped orifice between the left atrium and the cranial portion of the right atrium adjacent to the orifice of the SVC.

Once the defect is visualized from the right atrial perspective, the image is rotated along its vertical axis using the track ball to reveal the ostia of the right upper and the right middle pulmonary vein anomalously draining into the terminal portion of the SVC (Figures 8C and 8D, Video 8).

## DISCUSSION

ASDs usually develop through three mechanisms: (1) excessive resorption of an interatrial septal membrane that covers an ostium (e.g., partial or complete resorption of the septum primum in the region of the foramen ovale leading to ostium secundum ASDs), (2) persistence of an ostium that normally closes (e.g., ostium primum ASD), and (3) abnormal development (such as sinus venosus ASDs).

The two major objectives of this study were (1) to develop a standardized approach that all health care providers involved in image acquisition, interpretation, and clinical use can follow and (2) to place the 3D TEE images in an anatomically correct orientation. The protocol we propose takes only minutes to complete. Although there may be more rapid methods, any loss of time in orienting 3D TEE images using our method is rewarded by a standardized, anatomically correct

image orientation that facilitates interaction between echocardiographers, interventionalists, and cardiac surgeons. We believe that with a meticulous attention to detail, one can obtain 3D TEE images of the interatrial septum using the proposed technique.

In our laboratory, we have tried various approaches to orienting 3D TEE images of the interatrial septum and found out that the tilt-up approach from the opening scene provides on average more anatomic landmarks (the SVC, aorta, and even IVC and coronary sinus) than the tilt-down method (whose major anatomic landmarks are the fossa ovalis and occasionally the right upper pulmonary vein). In addition, the SVC with a clear distinction between its longitudinal and short axes appears to provide more orienting information than the much smaller and circular fossa ovalis.

Three-dimensional TEE imaging provides excellent real-time images of the interatrial septum and the atrial septum defects. It provides an en face view of the septum not obtainable by any other imaging modality in real time. For proper anatomic orientation of 3D TEE images of the interatrial septum and the atrial septum, we propose the TUPLE and ROLZ maneuvers. We hope that standardized maneuvers such TUPLE and ROLZ described in this article will enhance the diagnosis of ASDs and facilitate communication between echocardiographers obtaining 3D TEE images and interventional cardiologists or cardiac surgeons performing ASD closures.

## Limitations

Current 3D TEE systems suffer from several limitations. Occasionally, there is a dropout in the region of the fossa ovalis in both normal

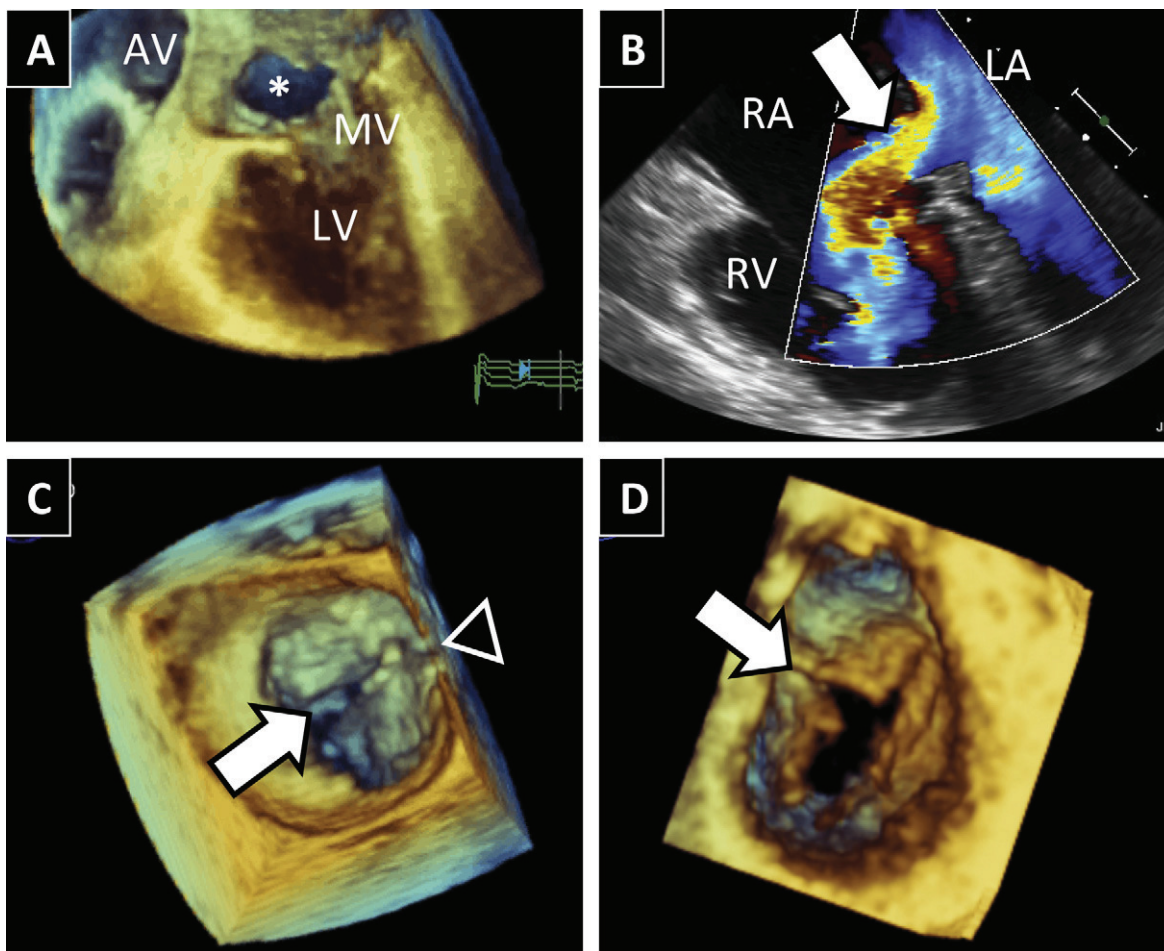


**Figure 7** Primum ASD. **(A)** The left atrial perspective of a primum ASD (asterisk) on a full-volume 3D TEE image. **(B)** A left-to-right shunt across the primum ASD (arrow) on a 2D color Doppler TEE image. **(C)** Three-dimensional zoom TEE image showing the left atrial aspect of the mitral valve (MV) having a cleft anterior leaflet (white arrow). The black arrowhead marks the location of the primum ASD. **(D)** Three-dimensional zoom TEE image showing the left ventricular aspect of the MV having a cleft anterior leaflet (arrow). AV, Aortic valve; LA, left atrium; LV, left ventricle; RA, right atrium; RV, right ventricle.

subjects and patients with ASDs. In normal subjects, the dropout creates the false appearance of an ASD. In patients with ASDs, the apparent ASD size may appear larger than it is in reality. The dropouts can be minimized by adequate gain controls and by the use of color Doppler (which demonstrates color flow through real septal defects but not through the dropouts). In addition, because the IVC enters the right atrium at different angles in different subjects, the inferior rim is sometimes hard to visualize and may represent a “blind spot.”

## REFERENCES

- Houck RC, Cooke JE, Gill EA. Live 3D echocardiography: a replacement for traditional 2D echocardiography? *AJR Am J Roentgenol* 2006;187:1092-106.
- Salcedo EE, Quaife RA, Seres T, Carroll JD. A framework for systematic characterization of the mitral valve by real-time three-dimensional transesophageal echocardiography. *J Am Soc Echocardiogr* 2009;22:1087-99.
- Sugeng L, Sherman SK, Salgo IS, Weinert L, Shook D, Raman J, et al. Live 3-dimensional transesophageal echocardiography initial experience using the fully-sampled matrix array probe. *J Am Coll Cardiol* 2008;52:446-9.
- Perk G, Ruiz C, Saric M, Kronzon I. Real-time three-dimensional transesophageal echocardiography in transcatheter, catheter-based procedures for repair of structural heart diseases. *Curr Cardiovasc Imaging Rep* 2009;2:363-74.
- McCarthy KP, Ho SY, Anderson RH. Defining the morphologic phenotypes of atrial septal defects and interatrial communications. *Images Paediatr Cardiol* 2003;15:1-24.
- Acar P, Saliba Z, Bonhoeffer P, Aggoun Y, Bonnet D, Sidi D, et al. Influence of atrial septal defect anatomy in patient selection and assessment of closure with the Cardioseal device; a three-dimensional transesophageal echocardiographic reconstruction. *Eur Heart J* 2000;21:573-81.
- Misra M, Sadiq A, Namboodiri N, Karunakaran J. The “aortic rim” recount: embolization of interatrial septal occluder into the main pulmonary artery bifurcation after atrial septal defect closure. *Interact Cardiovasc Thorac Surg* 2007;6:384-6.
- Taniguchi M, Akagi T, Watanabe N, Okamoto Y, Nakagawa K, Kijima Y, et al. Application of real-time three-dimensional transesophageal echocardiography using a matrix array probe for transcatheter closure of atrial septal defect. *J Am Soc Echocardiogr* 2009;22:1114-20.

733  
734  
735  
736  
737  
738  
739  
740  
741  
742  
743  
744  
745  
746  
747  
748  
749  
750  
751  
752  
753  
754  
755  
756  
757  
758  
759  
760  
761  
762  
763  
764  
765  
766  
767  
768  
769  
770  
771  
772  
773  
774  
775  
776  
777  
778  
779  
780  
781  
782  
783  
784  
785  
786  
787  
788  
789  
790  
791  
792  
793794  
795  
796  
797  
798  
799  
800  
801  
802  
803  
804  
805  
806  
807  
808  
809  
810  
811  
812  
813  
814  
815  
816  
817  
818  
819  
820  
821  
822  
823  
824  
825  
826  
827  
828  
829  
830  
831  
832  
833  
834  
835  
836  
837  
838  
839  
840  
841  
842  
843  
844  
845  
846  
847  
848  
849  
850  
851  
852  
853  
854

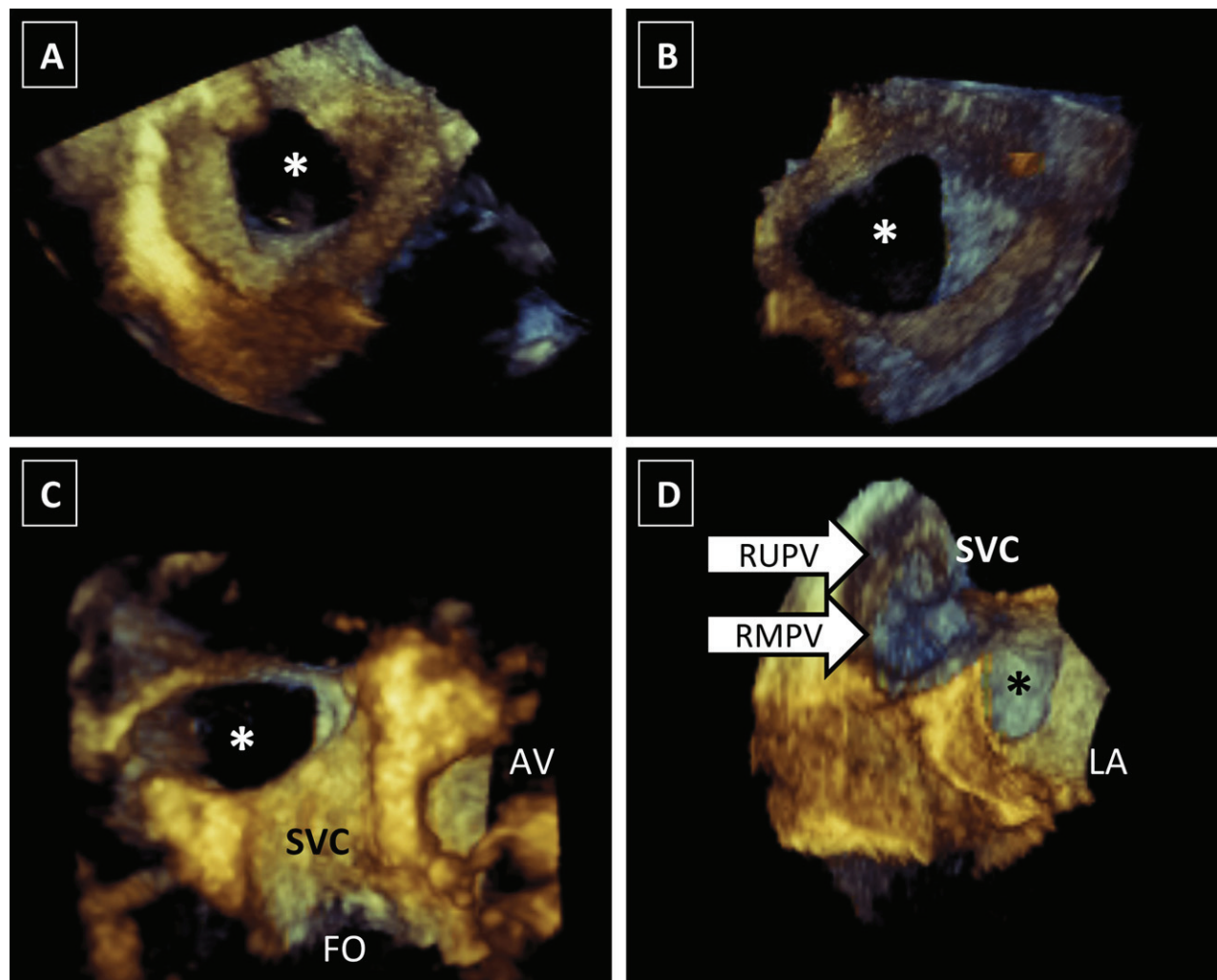


**Figure 8** SVC-type sinus venous ASD on 3D TEE imaging. **(A)** The right atrial aspect and **(B)** the left atrial (LA) aspect of an SVC-type sinus venous ASD (*asterisk*) visualized by the 3D zoom technique. **(C,D)** Full-volume 3D TEE images of another patient with an SVC-type sinus venous ASD (*asterisk*). **(C)** The right atrial aspect of the defect (*asterisk*). **(D)** The LA aspect of the defect (*asterisk*). The right upper pulmonary vein (RUPV) and right middle pulmonary vein (RMPV) drain anomalously into the SVC. AV, Aortic valve; FO, fossa ovalis.

**Video 1** Imaging of the normal interatrial septum using the TUPLE maneuver.

**Video 2** Imaging of the normal interatrial septum using the TUPLE and ROLZ maneuvers. This video was postprocessed using a source clip kindly provided by Dr. Robert Donnino of the Manhattan Campus of the Veterans Administration New York Harbor Healthcare System (New York, NY).

**Video 3** Imaging of a secundum ASD using the TUPLE maneuver.

**Video 4** Details of a secundum ASD.

**Video 5** Primum ASD.

**Video 6** Cleft mitral valve and primum ASD.

**Video 7** SVC-type sinus venous ASD.

**Video 8** Partial anomalous pulmonary venous return in a sinus venous ASD.



**AUTHOR QUERY FORM**

 <b>ELSEVIER</b>	<b>Journal:</b> YMJE  <b>Article Number:</b> 2303	
--	---	--

Dear Author,

Please check your proof carefully and mark all corrections at the appropriate place in the proof (e.g., by using on-screen annotation in the PDF file) or compile them in a separate list.

For correction or revision of any artwork, please consult <http://www.elsevier.com/artworkinstructions>.

Any queries or remarks that have arisen during the processing of your manuscript are listed below and highlighted by flags in the proof.

<b>Location in article</b>	<b>Query / Remark: click on the Q link to go Please insert your reply or correction at the corresponding line in the proof</b>
<b>Q1</b>	Your original reference 8 was a duplicate of reference 5 and was thus removed; the remaining reference was renumbered accordingly.

Thank you for your assistance.